

EFFECT OF TIP CLEARANCE ON THE PREDICTION OF NON-SYNCHRONOUS VIBRATIONS IN AXIAL COMPRESSORS

Martin Drolet[†]

École Polytechnique de Montréal
and Pratt & Whitney Canada
Longueuil, Québec, Canada

Huu Duc Vo

Njuki W. Mureithi
École Polytechnique de Montréal
Montréal, Québec, Canada

ABSTRACT

This work investigates the effect of tip clearance size and operating temperature on the predictions of the critical rotor speed at which Non-Synchronous Vibrations (NSV) can be encountered in a turbine engine axial flow compressor. It has been proposed that the tangential tip clearance flow, observed at high blade loading near stall, can act as an impinging resonant jet on the upcoming blades and could be the underlying physics behind NSV. A model, in the form of an equation to predict the critical blade tip speed at which NSV can occur, was proposed based on the Jet-Core Feedback Theory and was experimentally verified by Thomassin *et al.* [8]. In the equation, a factor k that was called the “tip instability convection coefficient” was measured experimentally and found to be influenced by the tip clearance size and operating temperature. This factor has a significant impact on the accuracy of the NSV predictions obtained using the proposed model.

This paper propose a numerical experiment to determine the effect of tip clearance size and temperature on k , in order to improve the critical NSV tip speed predictions using the proposed model. A review of the NSV model is presented along with the relevant background theory on the subject. Two different blade geometries are simulated to provide a generic approach to the study. The leakage flow velocity is calculated to estimate k and a correlation is proposed to model the behavior of the k parameter as a function of the tip clearance size. The latter was found to significantly improve the critical NSV speed predictions. The effect of operating temperature on k is also discussed. Finally, the variation of k with the aerodynamic loading is assessed and compared with available data in the literature to strengthen the generic nature of the results.

NOMENCLATURE

c	: Local speed of sound
C_a	: Mean axial velocity
CFD	: Computational fluid dynamics
EO	: Engine order (1,2,3,...)
f	: Frequency
FOR	: Frame of reference
h	: Tip clearance size
k	: Instability convection coefficient (U_{tip}/U_F)
LE	: Leading edge
M	: Mach number
n	: Harmonic integer number
N	: Rotor speed
NSV	: Non-synchronous vibrations
PS	: Pressure side
R_s	: Specific gas constant
s	: Blade pitch
St	: Strouhal number (reduced frequency)
SS	: Suction side
T	: Temperature
TE	: Trailing edge
U_{tip}	: Blade tip velocity
V_L	: Tip leakage flow velocity
W_{corr}	: Corrected air mass flow
γ	: Specific heat ratio
ϕ	: Flow coefficient
Ψ	: loading coefficient, pressure coefficient
ξ	: Hub-to-Tip ratio
ζ	: Chord length
σ	: Tip solidity (ζ_{tip}/s)
τ	: Non-dimensional tip clearance (h/ζ_{tip})

[†] Corresponding author: martin.drolet@polymtl.ca

Subscripts

- B,F : Backward, Forward wave in rotating frame
- b : Blade
- c : Speed of sound, Critical
- h,t : Hub, Tip

INTRODUCTION

Background Theory on Non-Synchronous Vibrations

Non-Synchronous Vibrations (NSV), along with classical flutter, are particular types of fluid-elastic instabilities that are part of the flow-induced vibrations (FIV) family observed in turbomachinery. Flow-induced vibrations are often the result of a coupling between the unsteady aerodynamic loading on a structure and the retroaction of the structure itself. Several NSV cases have been reported in the industry [1,2,3], in the front stages of axial compressors, but the physics behind NSV is yet to be fully understood.

Previous studies [2,4,5] have suggested that the tip clearance flow oscillations, that are known to occur at large tip clearance and high aerodynamic blade loading, could explain NSV. In addition, Vo [6] showed that these flow oscillations at the blade tip can occur when only one of the two criteria for spike-stall inception, namely the trailing edge tip clearance backflow [7], is satisfied. The tip clearance backflow and impingement on the adjacent blade pressure side is shown in Figure 1. Vo [6] thus suggested that these instabilities could arise from the impingement of the tip clearance flow leakage on the blade pressure side and that the study of the dynamics of impinging jets could explain NSV. An alternative tip clearance impingement flow path was also suggested later by Thomassin *et al.* [8], as shown by the dotted line in Figure 1.

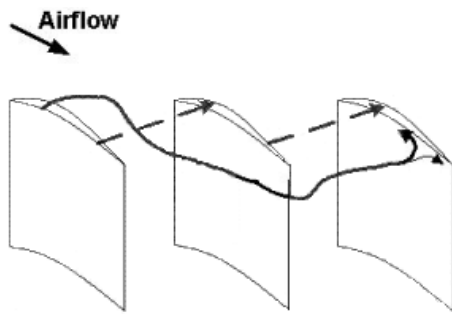


Figure 1: Tip clearance flow impingement flow paths [8]

Thomassin *et al.* [3,8] then proposed a physical mechanism that can explain and predict the critical speed at which NSV can occur for a given rotor geometry and operating conditions. Their NSV model was based on a jet-plate resonance analogy that they also developed, namely the jet core feedback theory [3], which is depicted in Figure 2 (a).

When a jet impinges on a flexible or vibrating plate, the vibration induces a pressure fluctuation at the stagnation point, in the jet centerline. This creates an acoustic pressure wave that

propagates back to the jet lip through the jet centerline at a velocity U_B . This implies that there exist a critical velocity $U_F = U_B - c$ where c is the local speed of sound. This can lead to a resonance when the ratio of the feedback wave velocity U_B to the feedback wavelength λ_B equals the natural frequency of the plate. This can be written, with the wavelength $\lambda_B = 2L/n$ to account for half wavelengths [3] as

$$f = f_b = St U_F / D = U_B / \lambda_B$$

Or,

$$f = f_b = n U_B / 2 L = n (c - U_F) / 2 L$$

where St is the jet Strouhal number, D is the jet diameter, L is the jet-to-plate distance, n is an integer to account for higher harmonics of the natural frequency and c is the local speed of sound.

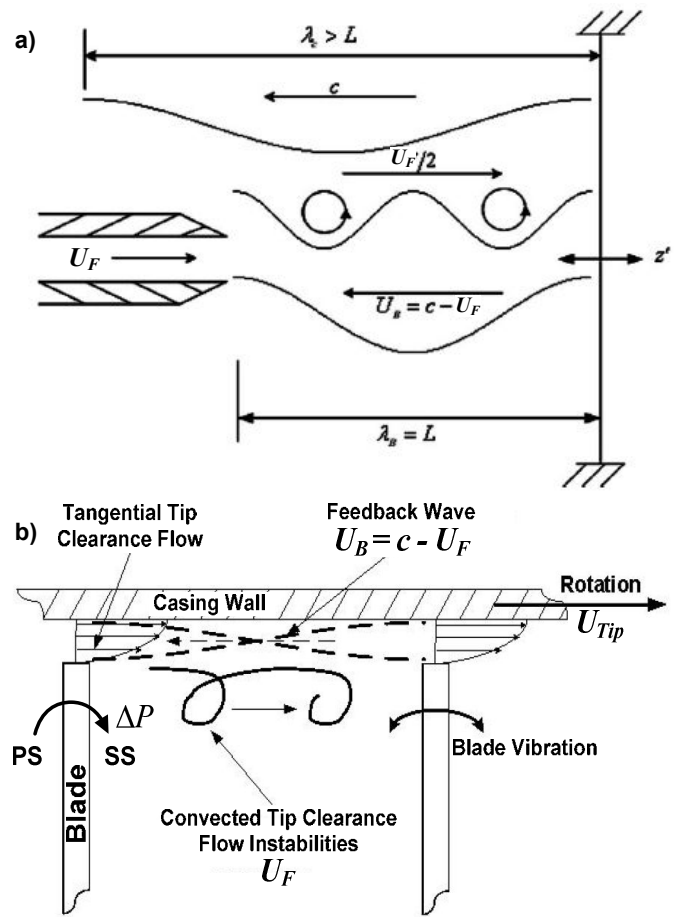


Figure 2: a) The jet core feedback theory [3] and b) physics of the proposed NSV model by Thomassin *et al.* [8]

The jet-core feedback theory was then applied to compressor blades by Thomassin *et al.* [3] as a possible mechanism for NSV. The analogy between the jet-core feedback flow and the compressor blade tip region flow is illustrated in Figure 2 (b) where the jet velocity U_F is now the tip clearance flow velocity. Structurally, the plate corresponds to the vibrating blade, the

jet-to-plate distance is the blade pitch, s , and the jet diameter is 2 times the tip clearance size, h , since the tip clearance flow profile is analogous to half of a jet profile.

The model suggests that, at particular operating conditions, the resonance of the tip clearance flow could be the physical mechanism linked with NSV [3,8]. These particular operating conditions are first, a high aerodynamic loading to get a tangential tip clearance flow that can act as an impinging jet (U_F) on the upcoming blades, as illustrated in Figure 1 and Figure 2 (b), and secondly, the proper operating temperature for the feedback wave (U_B) to have the corresponding wavelength to synchronize the tip clearance flow. This fluid-structure interaction can lead to the tip clearance flow resonance, which is believed to be the physical mechanism behind NSV [3,8,9].

Thomassin *et al.* [3] also derived an equation based on the jet-core feedback theory (eqn. 1), here shown as equation (2), to predict the critical blade tip speed at which NSV can occur.

$$U_{tipc} = 2 \left(c - \frac{2sf_b}{n} \right); \quad c = \sqrt{\gamma R_s T_{tip}} \quad (2)$$

where U_{tipc} is the critical blade tip speed, c is the tip local speed of sound, s is the blade pitch, f_b is the blade natural vibration frequency and n is an integer related to the harmonics of the acoustic feedback wave. The factor of 2 in front of the parentheses comes from the reported tip clearance flow velocity (U_F) that is known to be around half the blade tip speed during NSV [3,10,11], which led to the approximation $U_{tipc} \approx 2U_F$. The application of Thomassin's NSV model on the Campbell diagram is shown in Figure 3. The Campbell diagram is a tool used in compressor design to identify the coincidence of external excitation frequencies sources, such as forced responses and NSV, with the blade natural frequencies. The model of equation (2) appears on the diagram as the negative slope curves which can predict a range of possible NSV events for a given operational envelope.

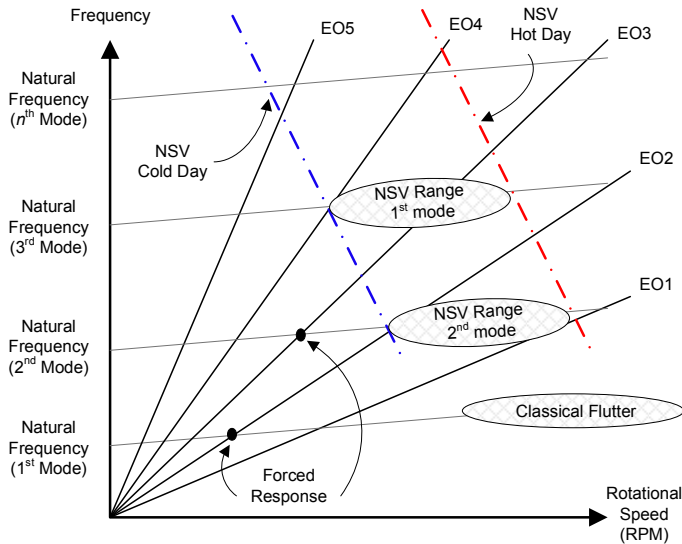


Figure 3: NSV prediction on Campbell diagram

Thomassin *et al.* [8] have also performed experiments on a rotor known to exhibit NSV to validate the proposed model. Two sets of three adjacent blades were instrumented with strain gauges and unsteady pressure sensors mounted on the blade tip. The results showed a resonance trend, both in stress and unsteady blade pressure measurements, that occurred around the predicted critical NSV speeds. Drolet *et al.* [9] have observed evidence of this resonance behavior using the unsteady pressure from numerical simulations with a moving blade mesh. Based on the simulations, they have also proposed a design methodology that uses numerical simulations to refine the critical NSV speed prediction and account for NSV in compressor design.

Thomassin *et al.* [8] found, based on their experiments, that the approximation $U_{tipc} \approx 2U_F$ used in their NSV model gives poor predictions of the critical NSV speed for particular conditions (up to $\sim 20\%$ error). Hence, they modified equation (2), using $U_{tipc} = kU_F$ as a more general form of the equation, which leads to

$$\frac{U_{tipc}}{\sqrt{T_{tip}}} = k \left(\sqrt{\gamma R_s} - \frac{2s f_b}{n \sqrt{T_{tip}}} \right) \quad (3)$$

$$\text{where } k = U_{tipc} / U_F \quad (4)$$

with U_F defined as the forward travelling wave convection velocity (or jet velocity) in the rotating frame of reference and U_{tip} is the blade tip speed. The factor k was defined as the “instability convection coefficient” [8] and was shown to have a large influence on the accuracy of the critical blade tip speed prediction (eqn. 3) at which NSV can occur [8, 9]. Thomassin *et al.*[8] have measured the instability convection coefficient (k) from their experiments for two inlet temperatures and two tip clearance sizes (presented here as percentage of the tip chord). The available data is plotted herein as a function of the corrected speed in Figure 4. With the proper value of k used in the model of equation (3), the critical NSV speed predictions were improved by up to a factor of 10 when compared to the initial approximation $U_{tipc} \approx 2U_F$. This suggests that this k parameter must be known for a given geometry in order to get accurate predictions for NSV using the proposed model.

In addition, it can be observed from Figure 4 that the measured [8] instability convection coefficient (k) appears to vary with tip clearance size. As the tip clearance size increases from 1% to 2% tip chord, it shows from the results that k changes respectively from an average of 1.96 to 1.67 (cold) and from 1.85 to 1.73 (hot). On the other hand, there are not enough data points to provide adequate statistics on the variation of k with temperature; there is a slight distinction between the cold and hot measurements, especially for the 2% case, however, the trends are not as clear in the case of 1% tip clearance.

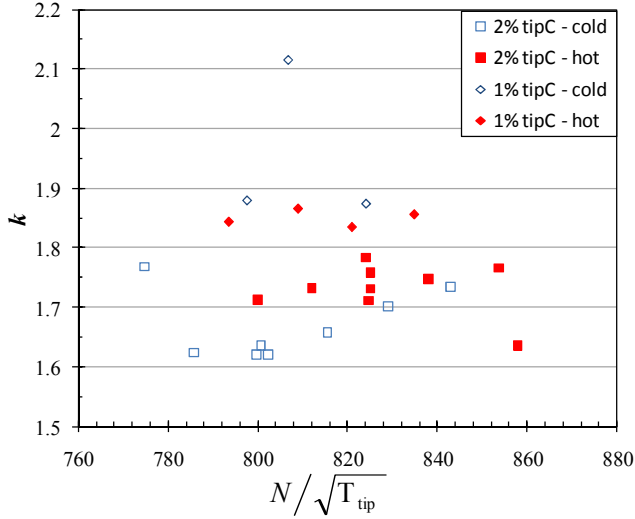


Figure 4: Measured instability convection coefficient, k , at different operating conditions, data from [8]

Since the parameter “ k ” must be known to accurately predict the critical NSV speed, it is therefore relevant to seek a correlation for the instability convection coefficient such that equation (3) can be used, independently from experimental tests and simulations, in the early design stages of compressor geometries to avoid non-synchronous vibrations in a given operating range.

Jet-Like Behavior of the Tip Clearance Flow

As previously mentioned, the model proposed by Thomassin *et al.* [3] is based on an impinging jet analogy. The impinging jet-like behavior of the tip clearance flow was suggested by Vo [6]. Storer and Cumpsty [14] have measured the tip leakage velocity, V_L , and also identified the jet-like behavior of the tip clearance flow. The leakage velocity is defined as the velocity component normal to the camber line [15] or, when the blade is thin, the velocity component normal to the blade surface can be used [14]. Thus, the leakage velocity (V_L) could possibly be used to estimate the “jet” velocity, U_F , in Thomassin’s model [3] and calculate the instability convection coefficient (k).

Overview of the Current Study

Previous numerical work on NSV has been reported in which the more fundamental details of the phenomenon were studied in order to elucidate the NSV mechanism [2,4,6] and, in other cases, a CFD-based predictive method was proposed [9,16]. The current study uses a CFD approach to investigate the effect of tip clearance size and operating temperature to refine the analytical prediction of the critical rotor speed at which NSV can occur, based on the mechanism proposed by Thomassin *et al.* [3,8]. Numerical simulations are performed at several tip clearance sizes and temperatures that are representative of typical engine operating conditions, with two different rotor geometries, in order to estimate the “jet” velocity, U_F . The specific objectives of the proposed work are,

first to assess the effect of tip clearance size and temperature on the behavior of the instability convection coefficient (k). The second objective is to ultimately derive a physics-based design model for the k coefficient that would be generic (independent of the blade geometry) and greatly improve the critical NSV speed predictions using equation (3) from Thomassin *et al.* [8]. This would make it possible to consider NSV in the very early stages of a compressor design. Finally, the third objective is to contribute to further understanding of the physical characteristics of the tip clearance flow relevant to NSV.

The paper is organized as follows: a short parametric study is first presented to address which parameters are expected to govern the k coefficient. Then, a detailed description of the numerical simulations and methodology used is given after which the results on the effect of tip clearance size and temperature on the instability convection coefficient are presented. A discussion of the results follows and a correlation for k is proposed. The latter is then validated with available experimental data in terms of critical NSV speed predictions. Relevant features of the tip clearance flow and the generic nature of the study are finally discussed and conclusions are drawn from the investigation.

PARAMETRIC CONSIDERATIONS ON THE INSTABILITY CONVECTION COEFFICIENT, k

Dimensional analysis was conducted in order to determine the parameters governing the k coefficient from a theoretical point of view. Considering the fluid mechanics associated with the jet-like behavior of the tip clearance flow [14] in the context of the proposed NSV model [8], one can expect that the velocity U_F , used to determine the instability convection coefficient, will be some function g_1 of the flow and geometry parameters:

$$U_F = g_1(\Delta P, U_{tip}, h, \zeta_{tip}, T_{tip}, \rho, T_{1,ref}) \quad (5)$$

In the relation above, ΔP is the pressure difference across the blade, U_{tip} is the blade tip speed, h is the tip clearance size, ζ_{tip} is the blade chord length at tip, U_F is the mean tip clearance flow velocity, T_{tip} is the average blade tip temperature, ρ is the fluid density and $T_{1,ref}$ is the (reference) inlet temperature, upstream of the rotor.

Taking ρ , U_{tip} , ζ_{tip} and $T_{1,ref}$ as the four repeating parameters, one can form the following dimensionless groups (Π):

$$\begin{aligned} \text{(a) } \Pi_1 &= \frac{U_F}{U_{tip}} = \frac{1}{k} & \text{(b) } \Pi_2 &= \frac{h}{\zeta_{tip}} \\ \text{(c) } \Pi_3 &= \frac{T_{tip}}{T_{1,ref}} \equiv T & \text{(d) } \Pi_4 &= \frac{\Delta P}{\rho U_{tip}^2} \end{aligned} \quad (6)$$

We now recognize that Π_1 is the reciprocal of the instability convection coefficient (k) and that Π_4 is equivalent to the loading or “pressure coefficient” that is defined as:

$$\psi = \frac{\Delta P}{1/2 \rho U_{tip}^2} \quad (7)$$

With Π_2 and Π_3 defined as the non-dimensional tip clearance (τ) and non-dimensional temperature (T), respectively, we can now write the instability convection coefficient “ k ” in terms of an arbitrary function G_1 of the other dimensionless groups which leads to equation (8).

$$k \equiv \frac{U_{tip}}{U_F} = G_1(\tau, T, \psi) \quad (8)$$

As previously discussed, NSV is expected to occur at high loading such as in conditions near stall. As will be argued later in the present paper, the blade loading ψ does not play an important role on the variations of the instability convection coefficient (k) in such conditions. Consequently, we can finally simplify the relation for “ k ” to:

$$k \equiv \frac{U_{tip}}{U_F} \approx G_2(\tau, T) \quad (9)$$

The latter puts forth the basic assumption considered in the present paper that the instability convection coefficient “ k ” will be mainly influenced by the tip clearance and operating temperature. This was also observed experimentally by Thomassin *et al.* [8], as previously discussed.

COMPUTATIONAL SET-UP

Methodology & Simulations

All simulations were performed using the commercial code ANSYS CFX (release 11.0) in steady-state mode using a k- ϵ turbulence model. The steady-state mode was chosen mainly to save on computation time, given the large number of simulations required for this study. Sample simulations near stall were verified in unsteady mode to ensure that there were no flow oscillations such that the choice of steady-state simulations would not affect the results. Two different geometries, one subsonic and one transonic, with, among other things, very different loading coefficient (ψ) near stall, were used in order to confer a generic approach to the study. Each geometry was investigated at six rotor speeds, every ~4% design speed ranging from 67% to 85%, which corresponds to the speed range investigated by Thomassin *et al.* [8]. To address the effect of tip clearance, six different tip clearance sizes, representative of typical values found in full engine configurations, were chosen and used for both geometries investigated. Since the tip chords of the two geometries are different, the dimensionless tip clearance provided a range of 0.5% to 4.8% of the tip chord and from 0.2% to 2.6% for the subsonic and transonic geometry, respectively.

The leakage velocity, V_L , was used to estimate the “jet” velocity, U_F , to find the instability convection coefficient, k , previously defined in equation (4). The leakage velocity used herein is defined in agreement with Rains [15] as being the velocity component normal to the camber line. The u and v

velocity components in the tip clearance flow were taken at ten equally spaced span-wise locations across the entire tip gap to find V_L which was area-averaged, over the tip clearance gap. This was repeated at ten chord-wise locations to cover the entire blade tip chord.

Geometry & Mesh Description

As previously mentioned, two different geometries were used, a subsonic rotor (low-speed/front-loaded) and a transonic rotor (high-speed/rear-loaded), which will be refer from now-on as SR and TR, respectively. A mesh study was performed on the TR geometry by Drolet *et al.* [9] and their simulations were validated with available experimental results. The mesh specifications used herein were thus selected based on their investigation. A detailed view of a typical mesh used is shown in Figure 5 for the SR geometry and in Figure 6 for the TR geometry.

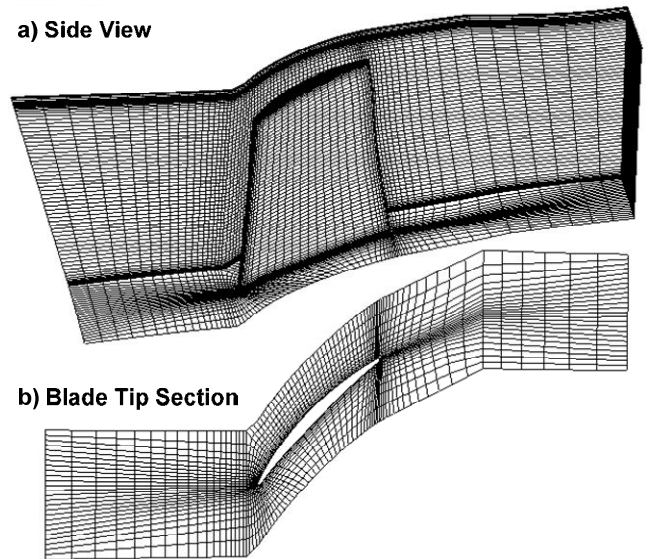


Figure 5: SR geometry a) Side view b) Blade tip section

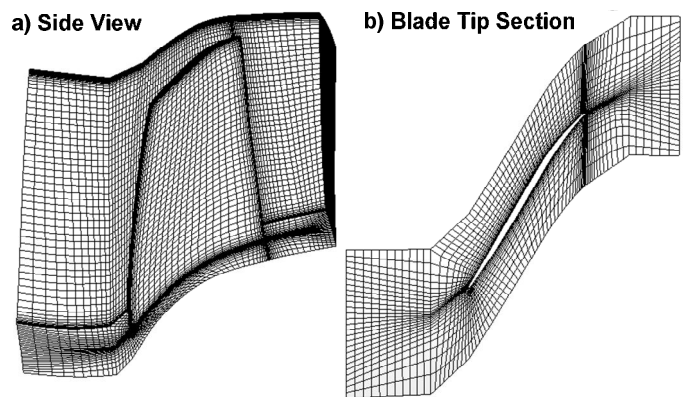


Figure 6: TR geometry a) Side view b) Blade tip section

Single-row, single-blade simulations were carried-out using a circumferential periodicity condition. An HJCL grid topology

was used, which allows for separate topology types in the upstream and downstream part of the computational domain, with approximately 250,000 nodes. In order to have adequate resolution of the radial distribution of the tip clearance flow velocity, the number of radial nodes in the tip region was always kept to a minimum of 12 nodes for small tip clearance sizes and increased for larger tip clearance sizes. This also ensured a y^+ value below 10 at the wall near the blade tip for all simulations. These two distinctive geometries were chosen for their different aerodynamic characteristics which could provide insights into the generic nature of the current study. The SR geometry has 45 blades with a tip solidity (σ) around 1.12, a hub-to-tip ratio (ξ) of approximately 0.8, a design flow coefficient (ϕ_{Design}) of 0.54 and a design total pressure ratio ($\text{PR}_{\text{Design}}$) of 1.41. The TR geometry is the same rotor geometry that was used by Thomassin *et al.* [8] in their experiment. It has 23 blades with $\sigma \approx 1.35$, $\xi \approx 0.47$, $\phi_{\text{Design}} = 0.48$ and $\text{PR}_{\text{Design}} = 1.79$.

Boundary Conditions

The boundary conditions used in the simulations consisted of specified total pressure, total temperature and swirl angle at the domain inlet and average static pressure at the domain exit. The wall portions in the domain were imposed a no-slip boundary conditions. The exit pressure was increased to obtain points along different speedlines to characterize both compressors and approach the near-stall conditions associated with NSV. To have a common base among all the simulations, they were brought near the stability limit region, using the spike-stall inception criteria as defined by Vo [18], which was considered as the near-stall region. It should be noted that when a static pressure boundary condition is used at the exit plane, solutions near stall cannot be calculated, should they fall beyond the peak total-to-static pressure rise characteristic of the compressor. This was the case for a few solutions for which the last converged condition, closest to stall, was used. All the simulations performed to assess the effect of tip clearance were set at ISA sea-level condition, which is also used herein as the reference inlet temperature ($T_{1,\text{ref}}$). To investigate the effect of temperature on k , three additional temperatures were used.

RESULTS AND DISCUSSION

Chord-wise Leakage Velocity Profiles

The tip leakage flow velocity, which is taken as the velocity component normal to the camber line as previously discussed, was calculated from the numerical simulations for all the different speed and tip clearances investigated. Examples of the chord-wise tip leakage velocity distribution, calculated at different rotor speeds, for the subsonic geometry at 1% tip clearance and for the transonic geometry at 0.4% tip clearance, are shown in Figure 7 (a) and (b), respectively. The data points in the figure were area-averaged over the entire tip clearance height, as previously explained. There is clearly a pattern that is

analogous to a jet in the first half portion of the blade chord, near the leading-edge.

A similar shape of the leakage flow was obtained by Storer and Cumpsty [14] except that the maximum leakage flow velocity in the jet-like profile was observed at mid-chord, which is most likely due to the loading conditions. In their case, the results were obtained at design conditions (closer to peak efficiency), where as in the present case, the results were calculated at very high blade loading (near stall). Also note that similar results, not shown here, were obtained for the other tip clearances investigated.

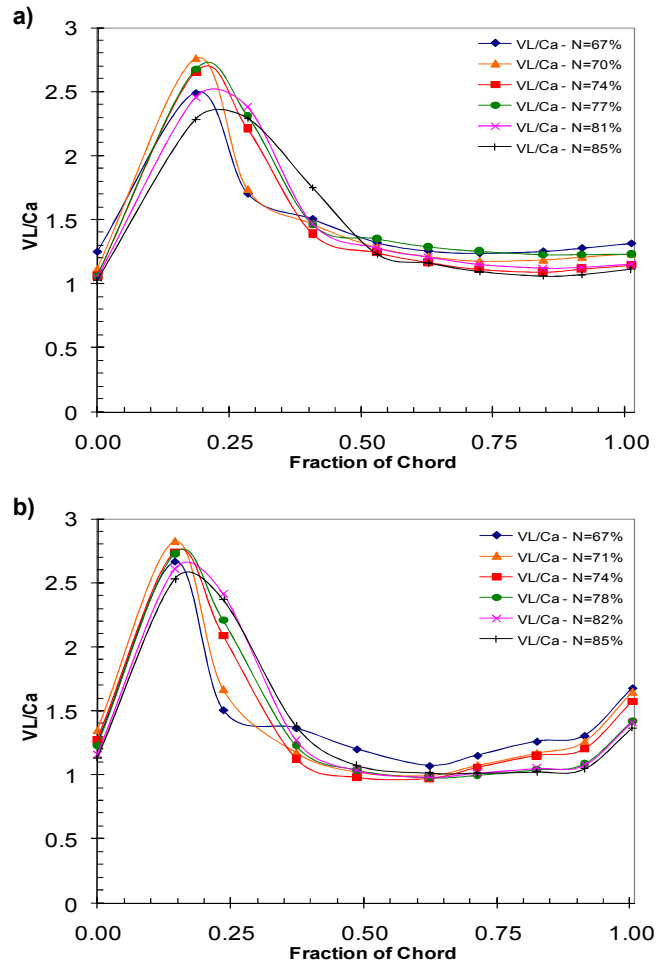
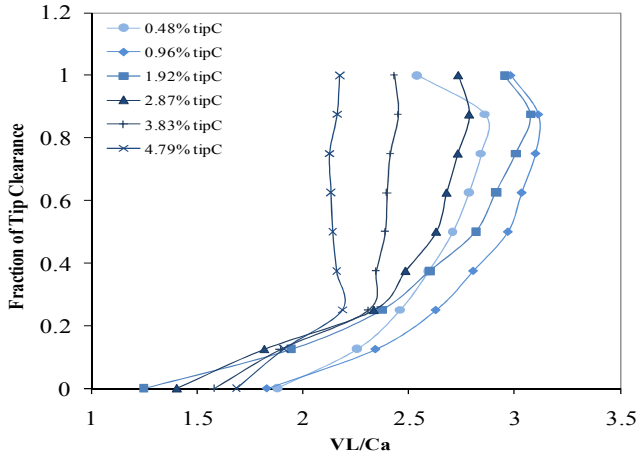


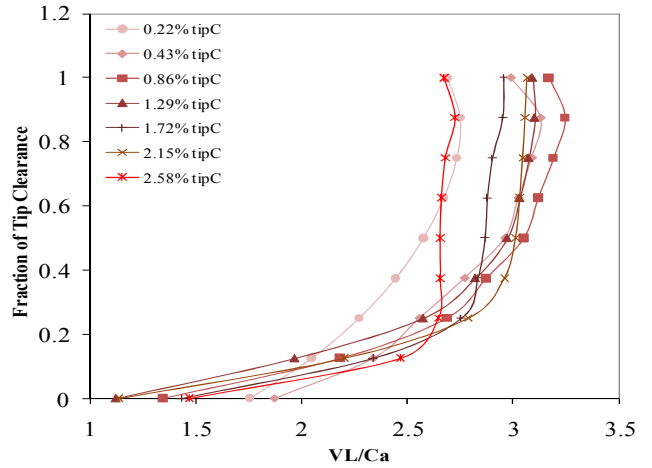
Figure 7: Typical chord-wise V_L profiles calculated at different rotor speeds for a) SR geometry at 1% chord tip clearance and b) TR geometry at 0.4% chord tip clearance

This jet-like pattern, observed in the first half portion of the chord for all simulated cases, could be possibly responsible for NSV following the resonant jet analogy proposed and experimentally verified by Thomassin *et al.* [3,8]. Consequently, for the purpose of the current study the “jet” velocity, U_F , is defined herein as per equation (10) in which ζ_{tip} is the tip chord length and $V_{L,\text{tip}}$ is the spanwise area-averaged V_L velocity component at chordwise location “ i ”.

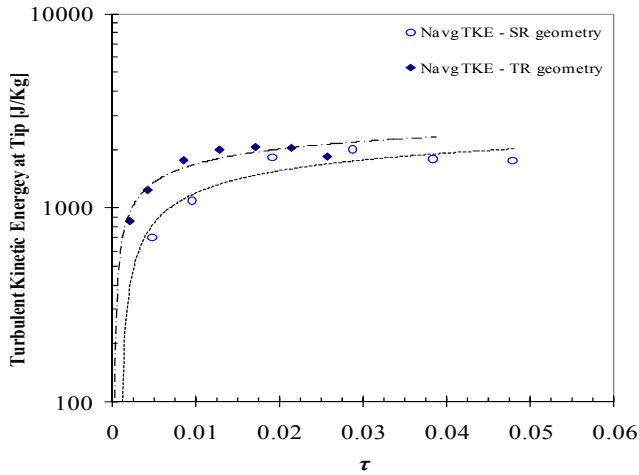
a) Tip leakage velocity profiles at 20% chord for SR geometry – N=70%



b) Tip leakage velocity profiles at 20% chord for TR geometry – N=71%



c) Area-averaged turbulent kinetic energy at tip for both geometries (N averaged)



d) Anticipated trend in k based on behavior of tip leakage flow velocity profiles

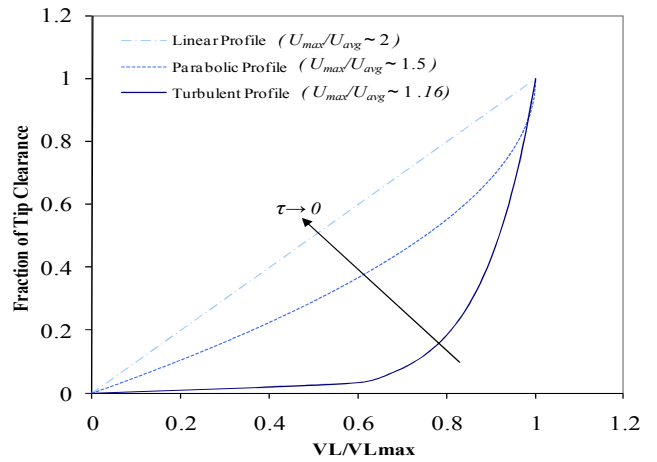


Figure 8: Characteristics of the tip leakage flow: Tip leakage velocity profiles for a) SR geometry and b) TR geometry, c) Area-averaged turbulent kinetic energy at tip averaged for all speed with logarithmic trend lines (dashed lines) and d) Anticipated trends in k with tip clearance based on velocity profiles behavior

$$U_F \equiv \frac{1}{\Delta \zeta_{tip}} \int_{\zeta_{tip,0}}^{\zeta_{tip,f}} \left(\overline{V_{L,tip}} \right)_i d\zeta_{tip} \quad (10)$$

The jet speed U_F used in Thomassin's model will be thus calculated from the area-averaged tip leakage velocity in the first half portion of the blade near the leading-edge, from 0 to 0.5 chord length.

U_F Velocity Profiles and Proposed Model for k vs τ

The velocity profile of the leakage flow across the tip gap was investigated near the center of the jet location, at around 20% of the chord, for all the different simulated tip clearances and speeds. An example of typical profiles that were calculated for the SR and TR geometries are shown in Figure 8 (a) and (b),

respectively. It can be observed, from the transonic rotor profiles (Figure 8(b)), that the velocity profile in the tip gap experiences a transition as the tip clearance is increased. At small tip clearances, the velocity profile is similar to that of a laminar boundary layer (0.22%, 0.43%, 0.86% and 1.29% chord tip clearances) before it finally reaches a fuller profile, similar to a turbulent boundary layer, at large clearances (1.72%, 2.15% and 2.58% chord tip clearances). A similar trend can be observed for the subsonic geometry as well.

The area-averaged turbulent kinetic energy was also calculated across the tip gap, and speed-averaged (N-averaged) for a given tip clearance, to assess the influence of the tip gap size and its contribution to turbulence. The results are shown here in Figure 8 (c). The logarithmic trend lines fitted through the results suggest that at very small tip clearances, there is very

low contribution of turbulent kinetic energy from the tip leakage flow and that its contribution rapidly increases before reaching an approximately constant value, once the tip leakage flow has become turbulent, at very large tip clearances. This also supports the previous observations regarding the laminar-to-turbulent profile transition observed in the tip leakage flow as the tip clearance increases.

Based on the observations regarding the tip leakage flow velocity profiles in the jet-like portion of the tip clearance flow, it is possible to anticipate the behavior of the instability convection coefficient, k . The latter was defined by Thomassin *et al.* [8] as the ratio of the blade tip speed over the jet speed, as shown in equation (4). This was based on the tip clearance flow velocity profile and is analogous, for any velocity profile, to the ratio of U_{max}/U_{avg} . Following this profile transition from turbulent to parabolic to linear as the tip clearance goes to zero, it is expected that the value of k should go from approximately 1.16 to 2 with an intermediate point around 1.5, which corresponds to typical values observed for theoretical turbulent, linear and parabolic velocity profiles, respectively. This relation is also depicted in Figure 8 (d). A correlation based on these physical trends will be thus used to model any relation between k and the variation in non-dimensional tip clearance (τ), as it will be discussed in the next sub-section. The correlation that will be used is based on a modified inverse tangent profile that can be written as

$$k(\tau) = \alpha \tan^{-1}[\beta(\tau_c - \tau)] + k_c \quad (11)$$

where τ_c and k_c represents the position of the inflection point in the inverse tangent profile. The coefficient α and β will be used to fit the proposed correlation to the numerical results.

Numerical Results on the Effect of Tip Clearance Size on k

The calculated values for the k coefficient for all the speeds and tip clearances investigated are shown in Figure 9. The standard deviation (in k) of the data varies from approximately 2% to 6%. This scatter in the data is possibly related to the variations in aerodynamic loading, which will be discussed later on, but there was no significant correlation between the different rotor speeds simulated and the variation of the data.

Figure 9 (b) shows the speed-averaged values of the calculated k for which the correlation of equation (11) was fitted. The values of τ_c and k_c used were 0.022 and 1.6, respectively. The correlation coefficients were found to be $\alpha = 0.265$ and $\beta = 300$ from a custom fitting model using the commercial MatLab software. This led to a goodness-of-fit of $r = 0.99$ and an rms error value of 3%. Available experimental data points of reported NSV cases are also shown in Figure 9 (b) for which the term “ k exact” is used as the exact value of k that would be required for equation (3) to perfectly predict the critical NSV speed. In addition, the “ k measured” from Thomassin *et al.*[8] are the values of k measured from

correlation between the casing and blade unsteady pressure measurements in their experiment.

It can be observed that both the (averaged) results from the numerical simulations and the available data from the literature show very good agreement with the proposed correlation model.

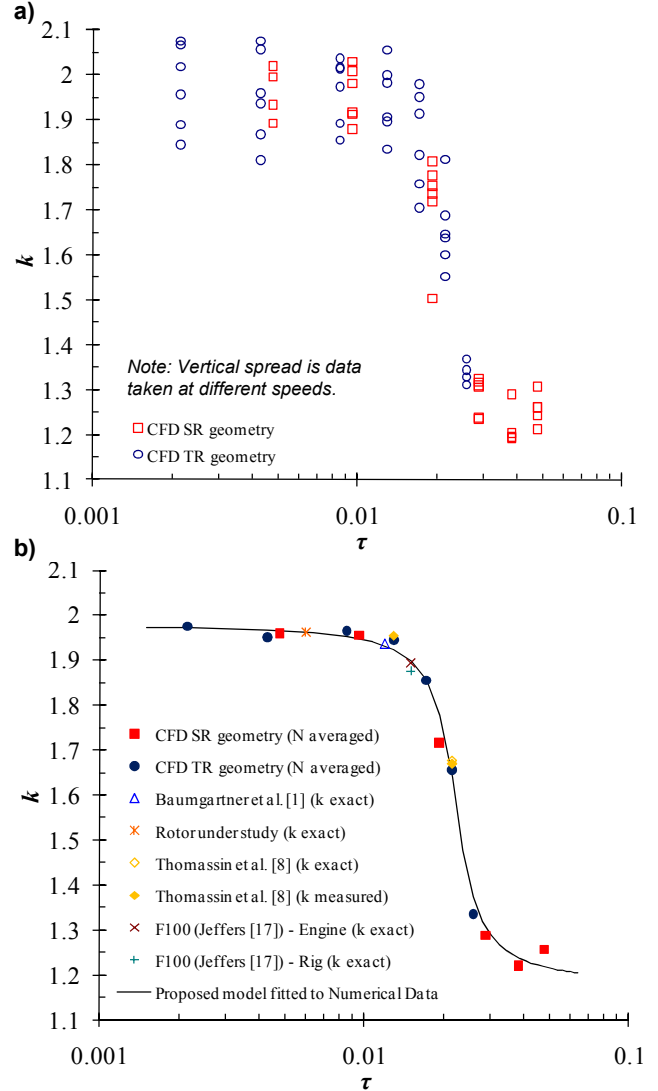


Figure 9: Numerical results for calculated k , a) Overall results, b) Comparison of available data in the literature with eqn. (11) fitted with speed-averaged numerical results

However, the value of k_c used in the correlation should have been ~ 1.5 according to the previous discussion on profile transition while the value that best-fitted the results was 1.6. In addition, the value of k should tend to ~ 1.16 at large non-dimensional tip clearance while the correlation that best-fitted the results actually tends to ~ 1.2 . One possible explanation for this small deviation at large non-dimensional tip clearance is that the velocity profile in the tip gap was found to be distorted at large tip clearance due to the roll-up of the tip clearance flow

near the blade suction side at the leading edge. In addition, this distortion of the velocity profile was mostly observed on the subsonic rotor geometry which has a much thicker blade profile at the tip when compared to the transonic geometry. Examples of distorted velocity profiles are shown in Figure 10 (a). This suggests that the vena-contracta effect, as shown by the ideal tip clearance flow model of Rains [15] in Figure 10 (b), is much more dominant when the blade thickness is large (relative to the tip clearance size) since the boundary layer has more time to develop and become more important in size relative to the tip gap size. This vena-contracta could thus affect the velocity profile near the tip and bias the value of k calculated which would result in a deviation from the expected value based on typical turbulent velocity profiles.

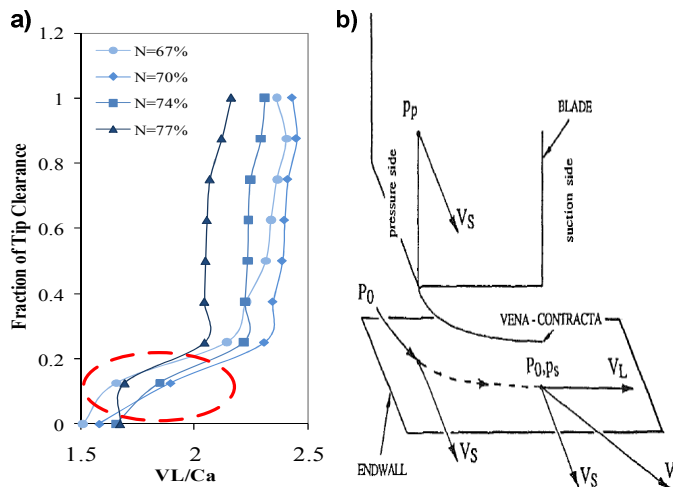


Figure 10: a) Distorted velocity profiles calculated at 3.83% tip clearance for the subsonic geometry and b) Ideal tip clearance flow model of Rains[15] as depicted in [14]

Numerical Results on the Effect of Temperature on k

Results from the previous sub-section on the effect of the tip clearance showed that there is little or no effect from the different blade geometries on the calculation of k . Hence, the effect of temperature was investigated only for the transonic rotor geometry at two different tip clearances, one small and one large, to save on computational time. Four temperatures were simulated to cover half of a typical engine design envelope. The results are shown in Figure 11 together with the average values experimentally obtained by Thomassin *et al.* [8]. The dashed lines are linear trend lines fitted to the data points.

The first thing to note from Figure 11 is that for both tip clearances calculated, there is a positive slope in the linear trend lines shown. The actual values of the slopes calculated were $dk/dT \approx 0.32$ and $dk/dT \approx 0.5$ for the 0.4% and 2% tip clearance, respectively. This is also consistent with that found by Thomassin *et al.* [8] for the 2% tip clearance case since both slopes calculated falls within that suggested by the experimental values, considering the measurement errors.

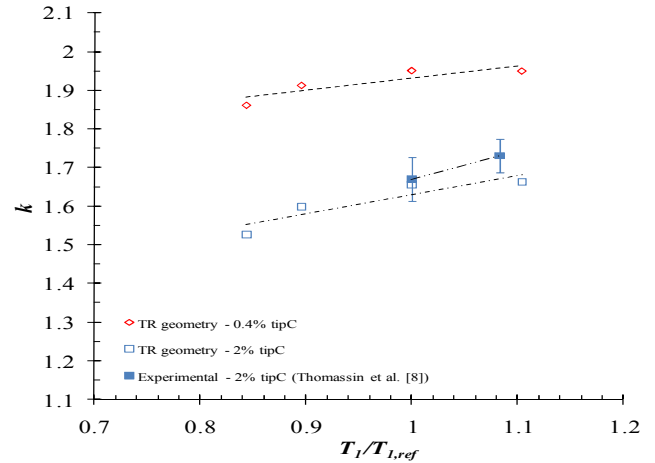


Figure 11: Calculated k at different inlet temperatures near stall for the TR geometry. Experimental data is from [8]

To summarize, the tip instability convection coefficient “ k ” was found to change with both tip clearance size and operating temperature from the numerical results, as also observed experimentally by [8]. However, the major contribution appeared to come from the change in tip clearance size and the change in “ k ” due to temperature can be neglected for preliminary design purposes.

Application of the Proposed Correlation to NSV Prediction

The correlation proposed in equation (11) and fitted to the numerical results (solid line in Figure 9 (b)) is used in equation (3) here to improved the critical NSV speed predictions, when compared to the general approximation of $k = 2$ used by Thomassin *et al.*[3]. The results for the different cases available in the literature are presented in Table 1. In the case of Baumgartner *et al.*[1], the exact tip clearance was unknown so a value of 1% of the tip chord was used in equation (11), which is a typical tip clearance size encountered in such engines. The inlet temperature of the F100 full engine case (Jeffers [17]) was unknown, although it was mentioned that the latter was at high Mach number flight conditions. A temperature ~ 1.2 times higher than the rig conditions, which was at sea level conditions, was thus used to predict k in this case.

The critical NSV speed predictions using the proposed correlation of equation (11) with $\tau_c = 0.022$, $k_c = 1.6$, $\alpha = 0.265$ and $\beta = 300$ shows very good agreement with the actual critical NSV speeds reported with a maximum error of 2.2%. The latter also shows a significant improvement from the value of $k = 2$ used by Thomassin *et al.*[3] which, for the same predictions, yielded errors between 2.0% and 19.8%.

Hence, the results suggest that the proposed correlation can be used to accurately predict the critical NSV speed for a given rotor geometry and operating conditions at the very early stages of the design process.

Table 1: Summary of critical NSV speed predictions

Reference Case	$U_{tip,c}$ [m/s]	$U_{tip,c}, k = 2$ (Thomassin <i>et al.</i> [3])	% error ($k = 2$)	$U_{tip,c}, k = k(\tau)$ (eqn. 11)	% error $k = k(\tau)$
Baumgartner <i>et al.</i> [1]	411.0	424.6	3.3	409.9	0.3
Rotor under study	329.5	335.7	2.0	329.5	0.0
Thomassin <i>et al.</i> [8] – cold T1	292.9	349.5	19.3	286.4	2.2
Thomassin <i>et al.</i> [8] – Hot T1	312.6	374.5	19.8	306.9	1.8
F100 (Jeffers [17]) - Rig	386.2	411.7	6.6	390.8	1.2
F100 (Jeffers [17]) – Full engine	380.0	401.2	5.6	380.8	0.2

Remarks on the Generic Nature of the Proposed Correlations

The current numerical study was conducted using two distinct geometries in the hope of finding a generic characteristic to the proposed correlations for k . The aerodynamic loading, calculated from the area-averaged static pressure on the blade pressure and suction sides, is shown in Figure 12 for the two geometries used and for all the tip clearances and different speeds that were simulated. The first thing to note from the figure is that the two geometries had different loading coefficients in the near-stall region investigated. In fact, the loading of the SR geometry was almost twice the loading of the TR geometry. However, all the simulations showed similar trends in k , which suggests that the correlations found for k should be independent of the loading. Given that compressors and fans can have different aerodynamic characteristics in terms of loading near stall, a theoretical analysis will be used below to complement the above numerical results in terms of assessing the generic nature of the correlation for “ k ” found previously.

Storer and Cumpsty [14] have developed a simple model for the tip clearance flow, based on the ideal flow model proposed by Rains [15], which was previously shown in Figure 10 (b). In their model, the tip clearance flow velocity (V) and its stream wise component (V_s) were mathematically represented as:

$$V = \sqrt{\frac{2(P_0 - p_s)}{\rho}} \quad (12)$$

$$V_s = \sqrt{\frac{2(P_0 - p_p)}{\rho}} \quad (13)$$

They ultimately found a relation for the tip leakage flow velocity (V_L), in terms of pressure coefficients, which can also be written as:

$$\frac{V_L}{U_{tip}} = \sqrt{\frac{(P_0 - p_p)}{1/2 \rho U_{tip}^2} - \frac{(P_0 - p_s)}{1/2 \rho U_{tip}^2}} = \sqrt{\frac{(p_p - p_s)}{1/2 \rho U_{tip}^2}} \quad (14)$$

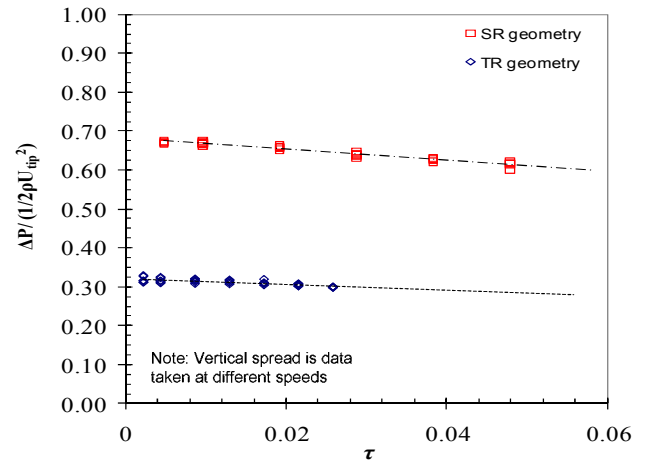


Figure 12: Calculated blade loading vs. non-dimensional tip clearance for both SR and TR geometries (data shown for all the different speeds)

Since V_L was used to calculate the jet velocity U_F , as previously defined by equation (10), we now realize that the instability convection coefficient “ k ” should be proportional to the inverse of equation (14). This relation, shown as equation (15), can thus approximate how k is expected to vary with the loading, ψ .

$$k \propto \frac{U_{tip}}{V_L} = \sqrt{\frac{1}{\psi}} \quad (15)$$

The relation found in equation (15) is plotted in Figure 13 (a) as a function of the loading. In conditions near stall, for which k was calculated to predict the critical NSV speed, the aerodynamic loading is typically high. Hence, one can expect from Figure 13 (a) that the value of k should show the smallest variations near stall since the slope of equation (15) tends to zero in such condition, as shown in Figure 13 (b).

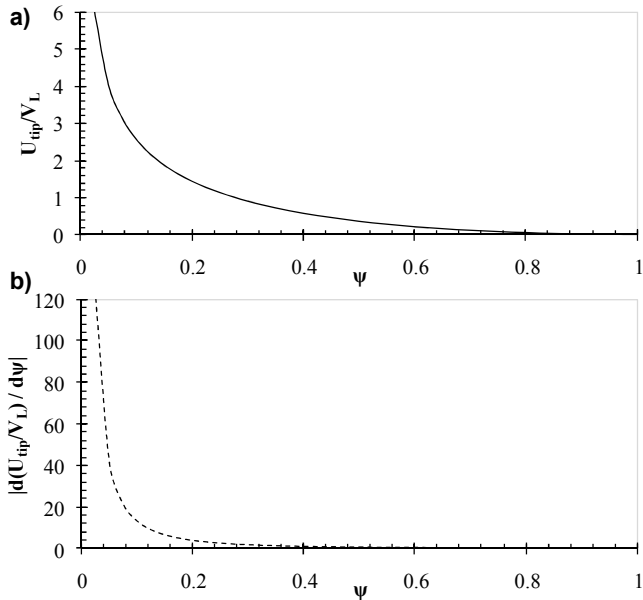


Figure 13: a) Equation (15) and its b) derivative plotted vs ψ

A brief literature survey was conducted to assess typical values of ϕ and ψ encountered in most compressors in order to validate the latter hypothesis. The results are shown in Figure 14, which clearly shows that most compressor will stall at a loading greater than 0.3.

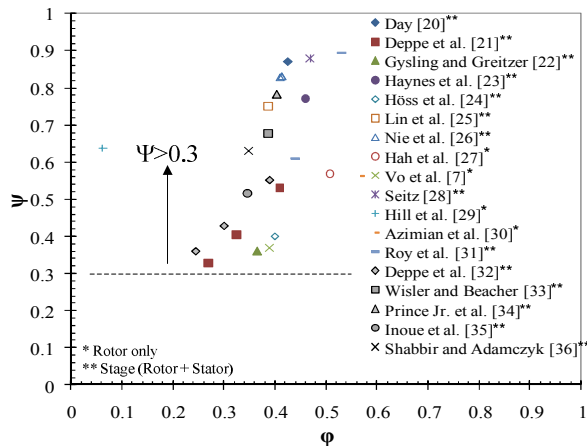


Figure 14: Typical values of loading, ψ , and flow coefficient, ϕ , found near stall for most compressor geometries

By looking at the variation in ψ of equation (15), a given value of k , taken at $\psi=0.6$, will show variations of $\pm 2\%$ from $\psi=0.3$ to $\psi=0.9$. The analytical formulation of equation (15) thus proves the near-invariance of k with blade shape near stall, which was also validated with available data from the literature. Consequently, for design purposes, the correlation proposed herein as equation (11) can be considered to be generic for any compressor geometry.

CONCLUSION

A numerical experiment was conducted in order to determine the effect of tip clearance size and operating temperature on the tip instability convection coefficient, k , used to predict the critical NSV speed. The latter was found to change with both tip clearance size and operating temperature, as observed experimentally from previous work [8]. However, the major contribution appeared to come from the change in tip clearance size and the contribution of the temperature effect was found negligible for preliminary design purposes.

A correlation was proposed to determine the k value as a function of the tip clearance size and was shown to significantly improve the critical NSV blade tip speed predictions, when applied to available data from the literature. The predictions were found to be within 0.0% and 2.2% of the actual NSV critical tip speed when the same predictions using the previous assumption of $k = 2$ [3] were between 2.0% and 19.8%. Additional discussion on the generic feature of the study was also presented and suggested that, based on typical values of flow coefficient and loading observed near stall from available data in the literature, the proposed correlation could be used for design purposes on any compressor geometry.

In summary, the current numerical study proposed a simple and generic correlation that greatly improves the analytical critical NSV speed predictions that can be used in the early design stages of axial compressors and fans.

ACKNOWLEDGMENTS

The authors would like to thank Pratt & Whitney Canada for supporting this research initiative and for the authorization to publish this work. The principal author would also like to express his personal thanks to Dr. Jean Thomassin for the numerous insightful discussions on non-synchronous vibrations.

REFERENCES

- [1] Baumgartner, M., Kamaler, F. and Hourmouziadis, J., "Non-Engine Order Blade Vibration in a High Pressure Compressor", ISABE Paper 95-7094, 1995.
- [2] Kielb, R.E., Thomas, J.P., Barter, J.W. and Hall, K.C., "Blade Excitation by Aerodynamic Instabilities – A Compressor Blade Study", ASME Paper GT-2003-38634, 2003.
- [3] Thomassin, J., Vo, H.D. and Mureithi, N.W., "Blade tip clearance flow and compressor NSV: The jet core feedback theory as the coupling mechanism", ASME Journal of Turbomachinery, vol. 131, Jan. 2009, DOI:10.1115/1.2812979.
- [4] März, J., Hah, C. and Neise, W., "An Experimental and Numerical Investigation Into the Mechanisms of Rotating Instability", ASME Journal of Turbomachinery, vol. 124, pp.367-375, July 2002.
- [5] Mailach, R., Lehmann, I. and Vogeler, K., "Rotating Instabilities in an Axial Compressor Originating from the Fluctuating Blade Tip Vortex", ASME Journal of Turbomachinery, vol.123, pp.453-463, July 2001.
- [6] Vo, H.D., "Role of Tip Clearance Flow in the Generation of Non-Synchronous Vibrations", AIAA Paper 2006-629,

Proceedings of the 44th AIAA Aerospace Sciences Meeting and Exhibit, Reno, Nevada, 2006.

[7] Vo, H.D., Tan, C.S. and Greitzer, E.M., “Criteria for Spike Initiated Rotating Stall”, ASME Journal of Turbomachinery, vol. 130, Jan. 2008, DOI:10.1115/1.2750674.

[8] Thomassin, J., Vo, H.D. and Mureithi, N.W., “Experimental Demonstration to the Tip Clearance Flow Resonance behind Compressor NSV”, proceedings of GT2008: ASME Turbo Expo 2008: Power for Land, Sea and Air, June 9-13, 2008, Berlin, Germany, GT2008-50303.

[9] Drolet, M., Thomassin, J., Vo, H.D. and Mureithi, N.W., “Numerical Investigation into Non-Synchronous Vibrations of Axial Flow Compressors by the Resonant Tip Clearance Flow”, proceedings of GT2009: ASME Turbo Expo 2009: Power for Land, Sea and Air, June 8-12, 2009, Orlando, Florida, USA, GT2009-59074.

[10] Kameier, F. and Neise, W., 1997, “Rotating Blade Flow Instability as a Source of Noise in Axial Turbomachines”, J. Sound Vib., 203(2), pp. 833–853.

[11] Kameier, F. and Neise, W., 1997, “Experimental Study of Tip Clearance Losses and Noise in Axial Turbomachines and Their Reduction”, ASME J. Turbomachinery, 119, pp. 460–471.

[12] Ho, C.-M. and Nosseir, S., “Dynamics of an Impinging Jet Part I: The Feedback Phenomena”, Journal of Fluid Mechanics, vol. 105, pp.119-142, 1981.

[13] Mailach, R., Sauer, H. and Vogeler, K., 2001, “The periodical Interaction of the Tip Clearance Flow in the Blade Rows of Axial Compressors”, Proceedings of the ASME Turbo Expo 2001, New Orleans, Louisiana, USA, 2001-GT-0299.

[14] Storer, J.A. and Cumpsty, N.A., “Tip Leakage Flow in Axial Compressors”, ASME Journal of Turbomachinery, vol. 113, April 1991, pp.252-259.

[15] Rains, D.A., 1954, “Tip Clearance Flows in Axial Flow Compressors and Pumps”, California Institute of Technology, Hydrodynamics and Mechanical Engineering Laboratories, Report No.5.

[16] Spiker, M.A., Kielb, R.E., Hall, K.C. and Thomas, J.P., “Efficient Design Method for Non-Synchronous Vibrations using Enforced Motion”, proceedings of GT2008: ASME Turbo Expo 2008: Power for Land, Sea and Air, June 9-13, 2008, Berlin, Germany, GT2008-50599.

[17] Jeffers, J.D., “Aeroelastic Thermal Effects”, AGARD Manual on Aeroelasticity in Axial Turbomachines, vol. 2 (No 298), pp.21(1)-21(6), 1988.

[18] Vo, H.D., “Role of Tip Clearance Flow on Axial Compressor Stability”, Ph.D. Thesis, MIT, 2001.

[19] Thomassin, J., “Modélisation des Vibrations Asynchrones d’aubes de compresseurs axiaux par la résonance de l’écoulement de jeu”, Ph.D. Thesis, École Polytechnique de Montréal, 2009.

[20] Day, I.J., “Stall Inception in Axial Flow Compressors”, ASME Journal of Turbomachinery, vol. 115, Jan. 1993.

[21] Deppe, A., Saathoff, H. and Stark, U., “Stall Inception Phenomena in three Single-Stage Low-Speed Axial Compressors”, 10th International Symposium on Transport

Phenomena and Dynamics of Rotating Machinery, Honolulu, Hawaii, March 7-11, 2004.

[22] Gysling, D.L. and Greitzer, E.M., “Dynamic Control of Rotating Stall in Axial Flow Compressors using Aeromechanical Feedback”, ASME Journal of Turbomachinery, vol. 117, July 1995.

[23] Haynes, J.M., Hendricks, G.J. and Epstein, A.H., “Active Stabilization of Rotating Stall in a Three-Stage Axial Compressor”, ASME Journal of Turbomachinery, vol. 116, April 1994.

[24] Höss, B., Leinhos, D. and Fottner, L., “Stall Inception in the Compressor System of a Turbofan Engine”, ASME Journal of Turbomachinery, vol. 122, Jan. 2000.

[25] Lin, F., Li, M. and Chen, J., “Long-to-Short Length-Scale Transition: A Stall Inception Phenomenon in an Axial Compressor with Inlet Distortion”, ASME Journal of Turbomachinery, vol. 128, Jan. 2006.

[26] Nie, C., Xu, G., Cheng, X. and Chen, J., “Micro Air Injection and its Unsteady Response in a Low-Speed Axial Compressor”, ASME Journal of Turbomachinery, vol. 124, Oct. 2002.

[27] Hah, C., Bergner, J. and Schiffer H.P., “Short Length-Scale Rotating Stall Inception in a Transonic Axial Compressor - Criteria and Mechanisms”, proceedings of GT2006: ASME Turbo Expo 2006: Power for Land, Sea and Air, May 8-11, 2006, Barcelona, Spain, GT2006-90045.

[28] Seitz, P.A., “Casing Treatment for Axial Flow Compressors”, Ph.D. Thesis, Department of Engineering, University of Cambridge, Cambridge, Massachusetts, April 1999.

[29] Hill, S.D., Elder, R.L. and McKenzie, “Application of Casing Treatment to an Industrial Axial-Flow Fan”, Proceedings of the Institution of Mechanical Engineers, vol.212, pp.225-233, 1998.

[30] Azimian, A.R., Elder, R.L. and McKenzie, A.B., “Application of Recess Vaned Casing Treatment to Axial Flow Fans”, ASME Journal of Turbomachinery, vol. 112, Jan. 1990.

[31] Roy, B., Chouhan, M. and Kaundinya K.V., “Experimental Study of Boundary Layer Control through Tip Injection on Straight and Swept Compressor Blades”, proceedings of GT2005: ASME Turbo Expo 2005: Power for Land, Sea and Air, June 6-9, 2005, Reno-Tahoe, Nevada, USA, GT2005-68304.

[32] Deppe, A., Saathoff, H. and Stark, U., “Spike-Type Stall Inception in Axial-Flow Compressors”, proceedings of the 6th European Conference on Turbomachinery, Fluid Dynamics and Thermodynamics, March 7-11, 2005, Lille, France.

[33] Wisler, D.C. and Beacher, B.F., “Improved Compressor Performance using Recessed Clearance (Trenches)”, AIAA Journal of Propulsion, vol. 5, no.4, pp.469-475, July-August 1989.

[34] Prince Jr., D.C., Wisler, D.C. and Hilvers, D.E., “Study of Casing Treatment Stall Margin Improvement Phenomena”, General Electric Company, NASA Report No. CR-134552, March 1974.

- [35] Inoue, M., Kuroumaru, M., Tanino, T. and Furukawa, M., “Propagation of Multiple Short-Length-Scale Stall Cells in an Axial Compressor Rotor”, ASME Journal of Turbomachinery, vol. 122, Jan. 2000.
- [36] Shabbir, A. and Adamczyk, J.J., “ Flow Mechanism for Stall Margin Improvement due to Circumferential Casing Grooves on Axial Compressors”, ASME Journal of Turbomachinery, vol. 127, Oct. 2005.
- [37] Cumpsty, N.A., “Compressor Aerodynamics”, Longman Group UK Limited, 1989.
- [38] Saravanamuttoo H.I.H., Rogers, G.F.C. and Cohen, H., “Gas Turbine Theory”, 5th edition, Pearson Prentice Hall, 2001.